



Available online at <http://scik.org>

Commun. Math. Biol. Neurosci. 2024, 2024:26

<https://doi.org/10.28919/cmbn/8382>

ISSN: 2052-2541

EFFECT OF NON-LINEAR HARVESTING AND DELAY ON A PREDATOR-PREY MODEL WITH BEDDINGTON-DEANGELIS FUNCTIONAL RESPONSE

MIQIN CHEN^{1,*}, WENSHENG YANG^{1,2}

¹School of Mathematics and Statistics, Fujian Normal University, Fuzhou 350117, Fujian, P. R. China

²FJKLMAA and Center for Applied Mathematics of Fujian province (FJNU), Fuzhou 350117, Fujian, P. R. China

Copyright © 2024 the author(s). This is an open access article distributed under the Creative Commons Attribution License, which permits unrestricted use, distribution, and reproduction in any medium, provided the original work is properly cited.

Abstract. The interaction of prey and predator is a critical issue in population dynamics modeling. In this paper, we investigate the dynamics of a delayed predator-prey model with Beddington-DeAngelis functional responses and non-linear harvesting of predators. Also, the fear of predators in prey species is introduced. In the absence of a time delay, the positivity, boundedness, stability of equilibrium points and local bifurcation of system are studied. From the analysis of the non-delayed model, we find that when the birth rate of prey is selected as the bifurcation parameter, the system undergoes a transcritical bifurcation at the trivial equilibrium point. Similarly, setting the bifurcation parameter to the maximum predation rate p resulted in a transcritical bifurcation at the predator-free equilibrium point. Furthermore, when the harvest effort value E is used as the bifurcation parameter, the system will have two Hopf bifurcation points close to the positive equilibrium point. In addition, the stability of the limit cycle generated by Hopf bifurcation is determined by calculating the first Lyapunov number. Our results show that fear of predation risk and harvest effort values can have stable and unstable effects. In addition, the predator mutual interference coefficient b may be responsible for the stability of the system. In the presence of a time delay, the time delay can also cause the system to generate limit cycles near the positive equilibrium point. Finally, some intriguing numerical simulation findings is provided in order to study the model's dynamics.

Keywords: non-linear harvesting; delayed prey-predator model; Beddington-DeAngelis functional response; transcritical bifurcation; Hopf bifurcation.

2020 AMS Subject Classification: 92D25, 92D40, 34D20.

*Corresponding author

E-mail address: 2050622812@qq.com

Received December 11, 2023

1. INTRODUCTION

The predator-prey model is an important mathematical model in population dynamics and an important study branch in the field of biomathematics. The first study on predator-prey dynamics was proposed by Lotka [1]. Numerous scholars have since expanded on Lotka's work [2-5]. Functional response plays an important role in the design and application of biological systems. During the last few decades, many researchers have used the Holling-type functional response to build their models. For instance, Holling [6] proposed the Holling type II functional response and it has been introduced and investigated by a large number of monographs on prey-predator models of bio-mathematics. Morozov [7] demonstrated that Holling type III functional response is suitable for investigating zooplankton feeding on algal blooms in deep-water ecosystems.

As we all know, Holling type functional response depends only on prey density. From a biological and ecological point of view, the Holling type functional response have been confronted with some challenges, see [8-10]. In some cases, many researchers in biology have claimed that the functional response comprised in a predator-prey system should be predator-dependent, such as when predators have to forage for food (and thus have to compete or share for food). Many important proofs show that functional responses associated with predator dependence are quite common in ecosystems [9,11-13]. In addition, a large number of experiments have shown that not only do predators interfere with each other's activities, thus producing a competitive effect, but also prey are threatened by the increased threat of predators and change their behavior. Consequently, models with predator dependence have more biological significance than models that depend on prey. In order to reconcile the theoretical and experimental views, Beddington [14] and DeAngelis et al. [15] considered the following form of functional response, $g(x,y) = \frac{px}{ax+by+c}$, which is similar to Holling type II functional response, but the additional term "by" in the denominator is interpreted as mutual interference between predators. Therefore, the traditional predator-prey ordinary differential system with Beddington-DeAngelis functional response can be presented as follows:

$$\begin{cases} \frac{dx}{dt} = rx - d_1x - \delta x^2 - \frac{pxy}{ax + by + c}, \\ \frac{dy}{dt} = -d_2y + \frac{upxy}{ax + by + c}, \end{cases} \quad (1.1)$$

where $x(t)$ and $y(t)$ represent the density of prey and predator populations at any time t respectively. r , d_1 , δ , d_2 and u are the birth rate of prey, the mortality rate of the prey, the prey intraspecific competition rate, death rate of predator, conversion rate of prey biomass to predator biomass, respectively. The functional form $\frac{px}{ax+by+c}$ is called Beddington-DeAngelis functional response, where p represents the maximum predation rate, a is prey interference rate, b is predator interference rate and c is the saturation constant. All parameters are positive. From a mathematical point of view, the general ratio-dependent and Holling type II systems can be considered as two special cases of the traditional Beddington-DeAngelis system. Compared with the ratio-dependent type, it has the same features in qualitative behavior but eliminates some singular features at lower densities. Therefore, in the present study, we are more interested in the effect of the additional term “ by ” in the Beddington-DeAngelis functional response on dynamics of the model.

However, all the functional responses only reflect the direct killing of prey, no matter how they are complicated. Due to the fear from a predator the song sparrows (*Melospiza melodia*) reduce 40 % in offspring reproduction shown by Zanette et al. [16]. Thus, the presence of any predator can affect the birth rate due to anti-predator behavior more powerfully than direct predation. Mathematically, the fear effect was first proposed by Wang et al. [17]. They reasoned that the fear of predation would reduce the prey population’s birth rate. They found that the fear effect has no effect on the stability dynamics of a prey-predator model with a Holling type I functional response. However, when considering the Holling type II functional response, fear may stabilize the periodic dynamics. After this work, many researchers studied different predator-prey models by incorporating the cost of fear in prey reproduction. The fear function $\phi(x, y) = \frac{1}{1+ky}$ is the most commonly used. Here k denotes the level of fear. Recently, Thirthar et al. [18] investigated a three-species food chain model in which the fear of predators is considered in prey species, and both prey and predator occur according to the Beddington-DeAngelis type functional response. They discovered that the fear k of predator may be responsible for the

system's stability. So, in this work, we will consider the fear effect on prey species to study its influence in the proposed predator-prey model.

On the other hand, as we know, to meet the necessary needs of human beings, harvesting is inevitable. For example, the fishery, forestry, and wildlife systems are examples of resources that are used by human society for commercial purposes. To study the effect of harvesting mathematically, different types of harvesting policies are used, which are (i) constant harvesting; $H(x, E) = C$, where C is suitable constant; (ii) linear harvesting; $H(x, E) = qEx$, where q is catchability constant and E is harvesting effort; (iii) non-linear harvesting $H(x, E) = \frac{qEx}{n_1E + n_2x}$, where n_1, n_2 are positive constants. It is observed that the linear harvesting function has some unrealistic features such as unbounded prey harvesting and stochastic search for prey. The above unrealistic features are eliminated in the non-linear harvesting function. Furthermore, nonlinear harvesting may result in more complex dynamic behavior of the system than linear harvesting. For instance, in [19], it has been shown that the predator-prey model with non-linear harvesting might have a rich bifurcation phenomenon. For this reason, in this paper, we will introduce nonlinear harvesting of predators as the object of study of system dynamics.

Motivated by the above statements, in this article, we will consider the following prey-predator model with the fear of predator in prey species, the Beddington-DeAngelis functional response, and the non-linear harvesting of predator. The prey-predator model is represented by the following two nonlinear ordinary differential equations:

$$\begin{cases} \frac{dx}{dt} = \frac{rx}{1+ky} - d_1x - \delta x^2 - \frac{pxy}{ax+by+c}, \\ \frac{dy}{dt} = -d_2y + \frac{upxy}{ax+by+c} - \frac{qEy}{n_1E+n_2y}. \end{cases} \quad (1.2)$$

In a real-life application, every organism needs a constant time lag to reproduce its new program. We assumed that the predator takes τ time lag for the gestation of prey and the rate of change of predator density depends on the density of prey, predator present at the previous τ time. Therefore, by introducing discrete time delay, the model system (1.2) becomes the following form:

$$\begin{cases} \frac{dx}{dt} = \frac{rx}{1+ky} - d_1x - \delta x^2 - \frac{pxy}{ax+by+c}, \\ \frac{dy}{dt} = -d_2y + \frac{upx(t-\tau)y(t-\tau)}{ax(t-\tau)+by(t-\tau)+c} - \frac{qEy}{n_1E+n_2y}, \end{cases} \quad (1.3)$$

with initial conditions:

$$x(\theta) > 0, \quad y(\theta) > 0, \quad \theta \in [-\tau, 0), \quad (1.4)$$

where $x(t)$ and $y(t)$ represent the density of prey and predator populations at any time t respectively. Obviously, all solutions of the system (1.3) with the initial conditions (1.4) are always bounded.

The main objective of this paper is to investigate predator-prey dynamic behavior by adding fear effect, nonlinear harvesting, and time delays to the model (1.1). We are particularly interested in investigating whether inter-predator interference, non-linear harvesting, fear effects and time delays have a significant effect on the dynamical behavior of the model. The rest of the paper is organized as follows. The basic dynamical results such as positivity and boundedness, the existence of the equilibria and their stability and local bifurcation of the non-delayed system are given in Section 2. In Section 3, we analyze the Hopf bifurcation of the model in the presence of time delays near the positive equilibrium point. All our analytical results are verified numerically using MATLAB in Section 4. Finally, based on the above discussion, we give some conclusions in Section 5.

2. DYNAMIC ANALYSIS OF SYSTEM (1.3) WITH $\tau=0$

In this section, we will first discuss the positivity and boundedness of the solution of the system, and then analyze the existence of the equilibrium point and stability of the non-delayed system.

2.1. Positivity and boundedness of the solution. The non-negativity and positivity of solutions are illustrated by the following theorem.

Theorem 2.1. *All the solutions of system, which start in R_+^2 , are always positive and bounded.*

Proof. Firstly, we want to prove that $(x(t), y(t)) \in R_+^2$ for all $t \in [0, +\infty)$. For system (1.2) with initial conditions $x(0) > 0, y(0) > 0$, we have

$$\begin{aligned} x(t) &= x(0) \exp \left\{ \int_0^t \left[\frac{r}{1+ky(s)} - d_1 - \delta x(s) - \frac{py(s)}{ax(s)+by(s)+c} \right] ds \right\}, \\ y(t) &= y(0) \exp \left\{ \int_0^t \left[-d_2 + \frac{upx(s)}{ax(s)+by(s)+c} - \frac{qE}{n_1E+n_2y(s)} \right] ds \right\}, \end{aligned}$$

which shows that all the solutions of system (1.2) are always positive for all $t \geq 0$.

Secondly, we will prove the boundedness of the solution. Let $x(t)$, $y(t)$ be the solution of the system (1.2), define the function $W(t) = x(t) + \frac{1}{u}y(t)$ and $\eta > 0$ be some constant. Then

$$\begin{aligned} \frac{dW}{dt} &= \frac{dx}{dt} + \frac{1}{u} \frac{dy}{dt}, \\ &= \frac{rx}{1+ky} - d_1x - \delta x^2 - \frac{d_2}{u}y - \frac{qEy}{u(n_1E + n_2y)}, \\ &\leq rx - d_1x - \delta x^2 - \frac{d_2}{u}y. \end{aligned}$$

Next,

$$\frac{dW}{dt} + \eta W \leq x(r - d_1 + \eta) - \delta x^2 + \frac{1}{u}(\eta - d_2)y.$$

Now, we choose $\eta \in (0, d_2)$. The maximum value of $x(r - d_1 + \eta) - \delta x^2$ is $\frac{(r - d_1 + \eta)^2}{4\delta}$. Then, we have

$$\frac{dW}{dt} + \eta W \leq \frac{(r - d_1 + \eta)^2}{4\delta} = \beta.$$

Therefore, applying differential inequality, for all $t \geq T \geq 0$, we obtain

$$0 \leq W(t) \leq \beta - (\beta - W(T))e^{-(t-T)}.$$

Thus, all solutions of system (1.2) enter into the region $D = \{(x, y) : 0 \leq W(x, y) \leq \beta\}$. This shows that every solution of the system (1.2) is bounded.

2.2. The existence of equilibrium points. In this subsection, we mainly discuss the sufficient conditions for the existence of equilibrium points of the system (1.2). The system (1.2) has the following equilibria by calculation:

- (i) The trivial equilibrium $E_0(0, 0)$ always exists.
- (ii) The predator-free equilibrium $E_1(\frac{r-d_1}{\delta}, 0)$.
- (iii) Now we analyze the existence of the positive equilibrium $E^*(x^*, y^*)$, where the expressions of x^* , y^* can be obtained by solving the following equations

$$\begin{aligned} \frac{r}{1+ky^*} - d_1 - \delta x^* - \frac{py^*}{ax^* + by^* + c} &= 0, \\ -d_2 + \frac{upx^*}{ax^* + by^* + c} - \frac{qE}{n_1E + n_2y^*} &= 0. \end{aligned} \tag{2.1}$$

From the second equation of Eq. (2.1), we solve that

$$x^* = \frac{\left(\frac{qE}{n_1E+n_2y^*} + d_2\right)(by^* + c)}{up - \left(\frac{qE}{n_1E+n_2y^*} + d_2\right)a},$$

provided $up - \left(\frac{qE}{n_1E+n_2y^*} + d_2\right)a > 0$ and y^* is the root of the equation

$$a_1y^{*5} + a_2y^{*4} + a_3y^{*3} + a_4y^{*2} + a_5y^* + a_6 = 0,$$

where

$$a_1 = b^2d_2\delta kn_2^2u,$$

$$a_2 = kad_2n_2^2(ad_2 - d_1bu - 2pu) + \delta b^2d_2n_2u(n_2 + 2Ekn_1) + \delta kbn_2u(Eqb + 2cd_2n_2) + kn_2^2pu^2(d_1b + p),$$

$$a_3 = a^2d_2^2n_2(n_2 + 2Ekn_1) + n_2^2pu^2(p + bd - br) - 2ad_2n_2(n_2pu - Eakq - bd_1n_2u + bn_2ru) + Eb^2\delta n_2^2u$$

$$- acd_1d_2kn_2^2u + 2Ekn_2pu(n_1pu + aq) + ckun_2^2(cd_2\delta + d_1pu) + E^2b^2\delta n_1u(d_2n_1 + d_2n_2 + kq)$$

$$+ Ekn_2u(2bcq\delta - abqd_1 - 4apd_2n_1) + 2Ebn_1n_2uk(d_1pu - d_1d_2 + 2d_2\delta),$$

$$a_4 = E^2a^2kq^2 + 2En_1n_2(a^2d_2^2 + p^2u^2) + cn_2^2u(d_2\delta + d_1p - pr) + 2E^2a^2d_2q(n_2 + kn_1) + \delta E^2b^2n_1u(q + d_2n_1)$$

$$+ Ebn_2u(-ad_1q + 2c\delta q + aqr) + 2Eun_1n_2(-2apd_2 + bud_1 - bpru - abd_1d_2 + 2bcd_2\delta + ard_2 + c^2d_2\delta k$$

$$+ cd_1kpu - acd_1d_2k) + E^2n_1^2u(bd_1kpu - 2d_2kp - abkd_1d_2 + 2E^2bck\delta d_2) + Equ(c^2k\delta n_2 - 2Eapkn_1$$

$$- ackn_2d_1 - Eabkn_1d_1 + 2Ebck\delta n_1),$$

$$a_5 = E^2a^2q^2 + E^2a^2n_1(d_2 + 2d_2q) + E^2n_1^2u(p^2u - bpr + bd_1pu + c^2d_2k\delta + cd_1kpu - 2apd_2$$

$$- abd_1d_2 + 2bcd_2\delta + abrd_2 - ackd_1d_2) + Equ(c^2n_2\delta - 2Eapn_2 - acd_1n_2 + acrn_2 - Eabd_1n_1 + 2Ebcq\delta$$

$$+ Eabrn_1 + Ekqc^2\delta$$

$$- Eackn_1d_1) + 2Eun_1n_2(c^2d_2\delta + cd_1pu - cpr - acd_1d_2 + acd_2r),$$

$$a_6 = c^2E^2\delta un_1(q + d_2n_1) + (r - d_1)E^2cun_1(ad_1n_1 + aq - n_1p).$$

Obviously, the system (1.2) has at least one positive equilibrium point when $a_6 < 0$. Because defining the parameter conditions required for the actual number of coexistence equilibrium points is challenging, we plotted the nullclines for varied harvesting effort values in figs. 1 and 2. It is discovered that when the parameters satisfy $a_6 > 0$, the system (1.2) will have different number of equilibrium points when E is varied. When $E < 0.4899$, the system (1.2) has two positive equilibrium points; when $E = 0.48949$, the system (1.2) has only one positive equilibrium point; when the value of E increase continuously, the system (1.2) has no positive

equilibrium point. However, when the parameter condition $a_6 < 0$ is satisfied, the system (1.2) has only one positive equilibrium point regardless of what value E takes.

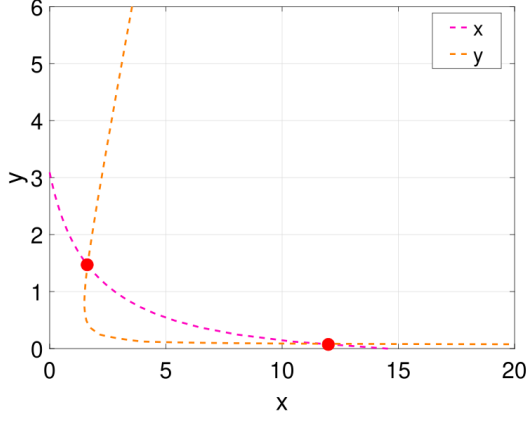
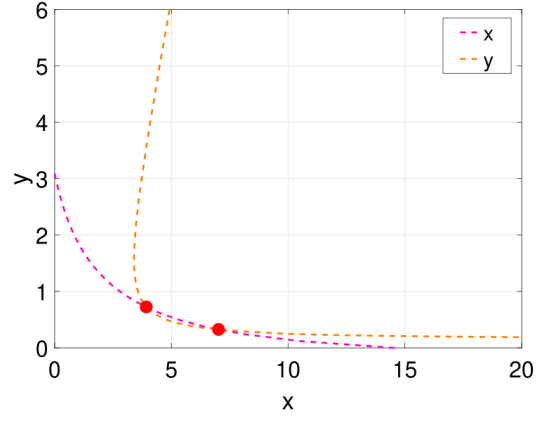
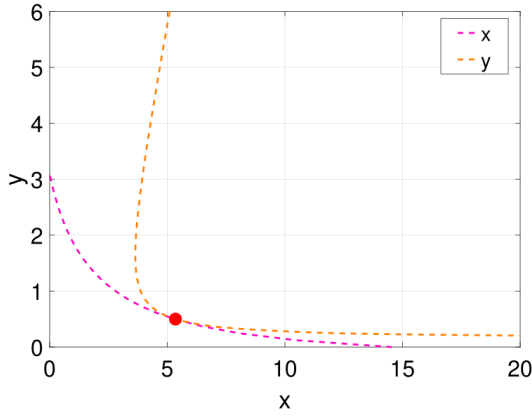
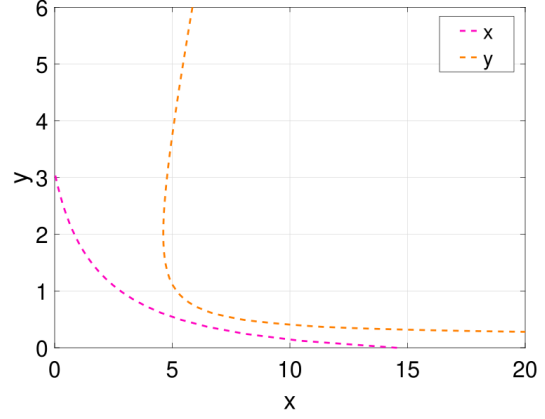
(A) $E = 0.15, a_6 > 0$ (B) $E = 0.45, a_6 > 0$ (C) $E = 0.48949, a_6 > 0$ (D) $E = 0.65, a_6 > 0$

FIGURE 1. Number of possible positive internal equilibrium points for different values of the harvesting effort E . Red dot denotes the equilibrium points, and the other parameter values are $r = 1.5, k = 3, d_1 = 0.05, \delta = 0.1, p = 0.3, a = 1, b = 2.8, c = 1, d_2 = 0.05, u = 1.2, q = 0.8, n_1 = 2, n_2 = 2$.

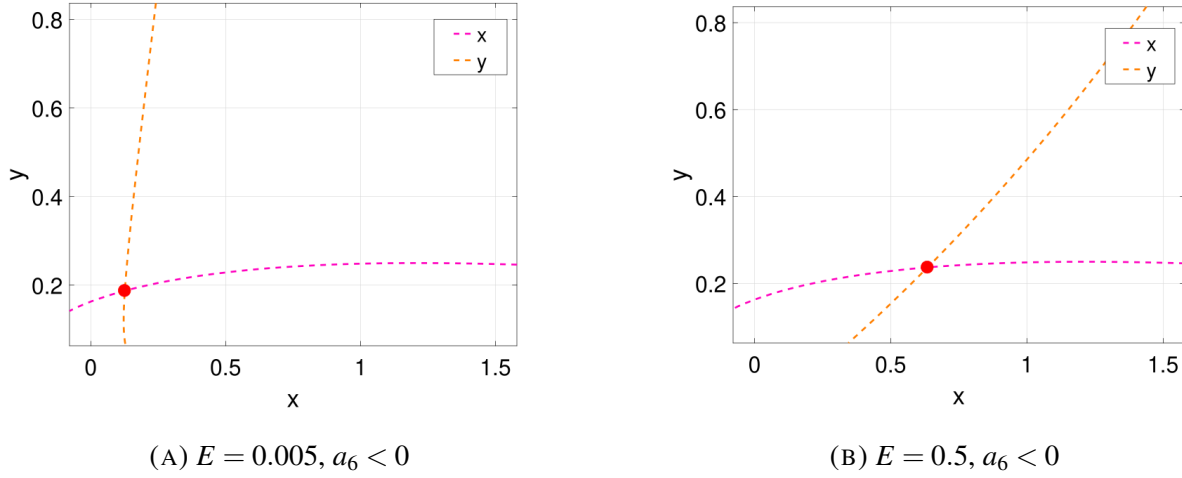


FIGURE 2. Number of possible positive internal equilibrium points for different values of the harvesting effort E . No matter what value E takes, the system (1.2) has only one positive equilibrium point when the parameter satisfies $a_6 < 0$. The other parameters are as follows: $r = 3, k = 30, d_1 = 0.05, \delta = 0.1, p = 2, a = 1.5, b = 2.5, c = 0.3, d_2 = 0.1, u = 0.7, q = 0.8, n_1 = 2, n_2 = 0.2$.

2.3. Stability of the equilibrium point. In this subsection, we discuss the stability property of the equilibrium points. First we compute the Jacobian matrix for system (1.2) to investigate the local stability of equilibria whenever they exist. $J(x, y)$ of system (1.2) at any point (x, y) is given by

$$J(x, y) = \begin{pmatrix} J_{11} & J_{12} \\ J_{21} & J_{22} \end{pmatrix},$$

where

$$\begin{aligned} J_{11} &= \frac{r}{1+ky} - d_1 - 2\delta x - \frac{py(by+c)}{(ax+by+c)^2}, \\ J_{12} &= \frac{-rkx}{(1+ky)^2} - \frac{px(ax+c)}{(ax+by+c)^2}, \\ J_{21} &= \frac{upy(by+c)}{(ax+by+c)^2}, \\ J_{22} &= -d_2 + \frac{upx(ax+c)}{(ax+by+c)^2} - \frac{n_1qE^2}{(n_1E+n_2y)^2}. \end{aligned}$$

The local stability is analyzed below by calculating the Jacobian matrix corresponding to each equilibrium point.

Accordingly, for the trivial equilibrium point E_0 , the Jacobian matrix takes the form as

$$J(E_0) = \begin{pmatrix} r - d_1 & 0 \\ 0 & -d_2 - \frac{q}{n_1} \end{pmatrix}.$$

The eigenvalues of $J(E_0)$ are $r - d_1$ and $-d_2 - \frac{q}{n_1} < 0$. Here, one eigenvalue is negative and other eigenvalue is negative if $r < d_1$. Hence trivial equilibrium point E_0 is stable if $r < d_1$ otherwise unstable. So we have the following theorem.

Theorem 2.2. *The trivial equilibrium E_0 is locally asymptotically stable if $r < d_1$ holds. Next, the Jacobian matrix of E_1 is given by*

$$J(E_1) = \begin{pmatrix} -(r - d_1) & -(r - d_1)\left(\frac{rk}{\delta} + \frac{p}{a(r - d_1) + \delta c}\right) \\ 0 & -d_2 + \frac{up(r - d_1)}{a(r - d_1) + \delta c} - \frac{q}{n_1} \end{pmatrix}.$$

The eigenvalues of the Jacobian matrix at E_1 are $-(r - d_1) < 0$ and $-d_2 + \frac{up(r - d_1)}{a(r - d_1) + \delta c} - \frac{q}{n_1}$. Since all parameter values are non-negative, the Predator-free equilibrium point E_1 is stable if $r < \frac{(\frac{q}{n_1} + d_2)\delta c}{up - a(\frac{q}{n_1} + d_2)} + d_1$ and unstable if $r > \frac{(\frac{q}{n_1} + d_2)\delta c}{up - a(\frac{q}{n_1} + d_2)} + d_1$. Based on the above discussion, we have the following Theorem.

Theorem 2.3. *Predator-free equilibrium point E_1 is locally asymptotically stable if $r < \frac{(\frac{q}{n_1} + d_2)\delta c}{up - a(\frac{q}{n_1} + d_2)} + d_1$ and saddle point for $r > \frac{(\frac{q}{n_1} + d_2)\delta c}{up - a(\frac{q}{n_1} + d_2)} + d_1$.*

Now, evaluating the Jacobian matrix of the model system (1.2) at positive equilibrium point $E^* = (x^*, y^*)$, we have

$$J(E^*) = \begin{pmatrix} J_{11}^* & J_{12}^* \\ J_{21}^* & J_{22}^* \end{pmatrix},$$

where

$$\begin{aligned} J_{11}^* &= -\delta x^* + \frac{apx^*y^*}{(ax^* + by^* + c)^2}, \\ J_{12}^* &= \frac{-rkx^*}{(1 + ky^*)^2} - \frac{px^*(ax^* + c)}{(ax^* + by^* + c)^2}, \\ J_{21}^* &= \frac{upy^*(by^* + c)}{(ax^* + by^* + c)^2}, \\ J_{22}^* &= \frac{qEn_2y^*}{(n_1E + n_2y^*)^2} - \frac{upbx^*y^*}{(ax^* + by^* + c)^2}. \end{aligned}$$

The characteristic equation around E^* is $\lambda^2 - Tr(J(E^*))\lambda + Det(J(E^*)) = 0$, where

$$Tr(J(E^*)) = J_{11}^* + J_{22}^*,$$

$$Det(J(E^*)) = J_{11}^*J_{22}^* - J_{12}^*J_{21}^*.$$

Now, if $Tr(J(E^*)) < 0$, and $Det(J(E^*)) > 0$, by using the Routh-Hurwitz criterion, all the eigenvalues of $J(E^*)$ have negative real part. According to the above discussion, we can obtain the following theorem.

Theorem 2.4. *The positive equilibrium point E^* is always locally asymptotically stable if $Tr(J(E^*)) < 0$ and $Det(J(E^*)) > 0$, otherwise it is unstable.*

2.4. Local bifurcation analysis. In this subsection, we shall discuss Transcritical bifurcation, Hopf bifurcation and the direction of Hopf bifurcation of the system (1.2). Here, we first discuss the transcritical bifurcation of the trivial equilibrium point $E_0(0,0)$, where the prey birth rate r is selected as the bifurcation parameter. Then, taking the maximum predation rate p as the bifurcation parameter, the same bifurcation occurs at the predator-free equilibrium point $E_1(\frac{r-d_1}{\delta}, 0)$.

Theorem 2.5. *The system (1.2) admits a transcritical bifurcation for $E_0(0,0)$ at the parameter $r = r^{[TC]} = d_1$.*

Proof. The jacobian matrix of the system (1.2) at the equilibrium point $E_0(0,0)$ for the parameter value $r = r^{[TC]} = d_1$ is

$$J(E_0; r = r^{[TC]}) = \begin{pmatrix} 0 & 0 \\ 0 & -d_2 - \frac{q}{n_1} \end{pmatrix}.$$

Obviously, the above jacobian matrix have a zero eigenvalue. Now, we find eigenvectors of the above jacobian matrix corresponding the zero eigenvalue. Eigenvectors of the jacobian matrix and its transpose matrix are $V = (1, 0)^T$ and $W = (1, 0)^T$. Now, we use the Sotomayor's theorem for transcritical bifurcation, then the transversality condition are

$$W^T F_r(E_0; r = r^{[TC]}) = 0,$$

$$W^T D F_r(E_0; r = r^{[TC]}) V = 1 \neq 0,$$

$$W^T D^2 F_r(E_0; r = r^{[TC]})(V, V) = -2\delta - 2rk - \frac{3p}{c} \neq 0.$$

Since all the transversality conditions are satisfied, the system (1.2) undergoes a transcritical bifurcation at $r = r^{[TC]}$. From a biological point of view, it is of great significance to analyze transcritical bifurcation. In this instance, the system has a suitable prey birth rate value below which both species are extinct; however, once the prey growth rate is crossed, only the prey species will survive.

Theorem 2.6. *The system (1.2) admits a transcritical bifurcation for $E_1(\frac{r-d_1}{\delta}, 0)$ at the parameter $p = p^{[TC]} = \frac{(\frac{q}{n_1} + d_2)(a(r-d_1) + \delta c)}{u(r-d_1)}$.*

Proof. The jacobian matrix of the system (1.2) at the equilibrium point $E_1(\frac{r-d_1}{\delta}, 0)$ for the parameter value $p = p^{[TC]} = \frac{(\frac{q}{n_1} + d_2)(a(r-d_1) + \delta c)}{u(r-d_1)}$ is

$$J(E_1; p = p^{[TC]}) = \begin{pmatrix} -(r-d_1) & -(r-d_1)(\frac{rk}{\delta} + \frac{p}{a(r-d_1) + \delta c}) \\ 0 & 0 \end{pmatrix}.$$

Obviously, $J(E_1; p = p^{[TC]})$ has a zero eigenvalue at $p = p^{[TC]}$. Now, the eigenvectors corresponding to the zero eigenvalue of the matrices $J(E_1; p = p^{[TC]})$ and $J(E_1; p = p^{[TC]})^T$, respectively, are given by $V = (\frac{-rk}{\delta} - \frac{\frac{q}{n_1} + d_2}{u(r-d_1)}, 1)^T$ and $W = (0, 1)^T$. Similarly, we use the Sotomayor's theorem for transcritical bifurcation, then the transversality condition are

$$W^T F_p(E_1; p = p^{[TC]}) = 0,$$

$$W^T DF_p(E_1; p = p^{[TC]})V = \frac{r-d_1}{a(r-d_1) + \delta c} \neq 0,$$

$$W^T D^2 F_p(E_1; p = p^{[TC]})(V, V) = -\frac{\delta x r k (\frac{q}{n_1} + d_2)}{(r-d_1)(a(r-d_1) + \delta c)} - \frac{\delta^2 c (\frac{q}{n_1} + d_2)^2}{u(r-d_1)^2 (a(r-d_1) + \delta c)} \neq 0.$$

Thus, again by Sotomayor's theorem, the system attains a transcritical bifurcation around the Predator-free equilibrium point E_1 at $p = p^{[TC]} = \frac{(\frac{q}{n_1} + d_2)(a(r-d_1) + \delta c)}{u(r-d_1)}$.

In the remainder of this section, we investigate for the possibility of Hopf bifurcation at the interior equilibrium E^* by taking the harvesting effort parameter E as the bifurcating parameter and keeping all the other parameters fixed. Define $\mu_1 = Tr(J(E^*))$, $\mu_2 = Det(J(E^*))$. Select E as the hopf bifurcation parameter if there exists $E = E_{HB}$, such that $H_1 : tr(J(E^*))|_{E=E_{HB}} = 0$ and $det(J(E^*))|_{E=E_{HB}} > 0$, $2\mu_1' \mu_2 + \mu_1 \mu_2' \neq 0$ holds, where μ_1' and μ_2' denote the derivatives of μ_1 and μ_2 with respect to E , respectively.

Theorem 2.7. *Assume that condition H_1 holds. When $E = E_{HB}$, the system (1.2) undergoes a*

Hopf bifurcation at the positive equilibrium point E^ .*

Proof. The Jacobian the characteristic equationmatrix at the positive equilibrium point E^* corresponds to the following characteristic equations

$$\lambda^2 - \mu_1\lambda + \mu_2 = 0. \quad (2.2)$$

When $E = E_{HB}$, $\mu_1 = 0$, the characteristic equation (2.2) can be described as

$$\lambda^2 + \mu_2 = 0, \quad (2.3)$$

then, equation (2.3) will have a pair of purely imaginary roots as $\lambda_1 = i\sqrt{\mu_2}$, $\lambda_2 = -i\sqrt{\mu_2}$. Next, differentiating the characteristic equation (2.2) with respect to E , we will obtain

$$2\lambda \frac{d\lambda}{dE} - \lambda\mu_1' - \frac{d\lambda}{dE}\mu_1 + \mu_2' = 0, \quad (2.4)$$

rectifying the equation (2.4) we can get

$$\frac{d\lambda}{dE} = \frac{\lambda\mu_1' - \mu_2'}{2\lambda - \mu_1},$$

then,

$$\left. \frac{d\lambda}{dE} \right|_{\lambda=i\sqrt{\mu_2}} = \frac{2\mu_1'\mu_2 + \mu_1\mu_2'}{4\mu_2 + \mu_1^2} + i \left[\frac{2\sqrt{\mu_2}\mu_2' - \mu_1\sqrt{\mu_2}\mu_2'}{4\mu_2 + \mu_1^2} \right],$$

consequently,

$$\operatorname{Re} \left(\frac{d\lambda}{dE} \right) \Big|_{\lambda=i\sqrt{\mu_2}} = \frac{2\mu_1'\mu_2 + \mu_1\mu_2'}{4\mu_2 + \mu_1^2} \neq 0.$$

Thus, we know that system (1.2) undergoes a Hopf-bifurcation at E^* as E passes through value E_{HB} .

Next, we calculate the first Lyapunov number σ at the system (1.2) positive equilibrium point E^* to further explore the nature of the limit cycle.

First, we transform the equilibrium point $E^* = (x^*, y^*)$ of the system (1.2) into the origin by letting $u = x - x^*$, $v = y - y^*$. The system (1.2) reduces to

$$\begin{aligned} \frac{du}{dt} &= a_{10}u + a_{01}v + a_{11}uv + a_{20}u^2 + a_{02}v^2 + a_{30}u^3 + a_{21}u^2v + a_{12}uv^2 + a_{03}v^3 + P(u, v), \\ \frac{dv}{dt} &= b_{10}u + b_{01}v + b_{11}uv + b_{20}u^2 + b_{02}v^2 + b_{30}u^3 + b_{21}u^2v + b_{12}uv^2 + b_{03}v^3 + Q(u, v), \end{aligned}$$

where

$$\begin{aligned}
a_{10} &= \frac{r}{1+ky^*} - d_1 - 2\delta x^* - \frac{py^*(by^*+c)}{(ax^*+by^*+c)^2}, & a_{01} &= \frac{-rkx^*}{(1+ky^*)^2} - \frac{px^*(ax^*+c)}{(ax^*+by^*+c)^2}, \\
a_{20} &= -\delta - \frac{2apx^*+pc}{2(ax^*+by^*+c)^2} + \frac{pax^*(ax^*+c)}{(ax^*+by^*+c)^3}, & a_{11} &= \frac{-rk}{(1+ky^*)^2} - \frac{2pby^*+pc}{(ax^*+by^*+c)^2} + \frac{2pby^*(by^*+c)}{(ax^*+by^*+c)^3}, \\
a_{02} &= \frac{rk^2x^*}{2(1+ky^*)} + \frac{pbx^*(ax^*+c)}{2(ax^*+by^*+c)^3}, & a_{21} &= \frac{b(apx^*+pc)}{2(ax^*+by^*+c)^3} - \frac{3pbx^*(ax^*+c)}{2(ax^*+by^*+c)^4}, \\
a_{30} &= \frac{-apx^*}{6(ax^*+by^*+c)^2} - \frac{a(2apx^*+pc)}{(ax^*+by^*+c)^3} + \frac{2a^2px^*}{(ax^*+by^*+c)^3} - \frac{a^2px^*(ax^*+c)}{2(ax^*+by^*+c)^4}, \\
a_{12} &= \frac{rk^2}{2(1+ky^*)^4} - \frac{pb}{(ax^*+by^*+c)^2} + \frac{b(2pby^*+pc)}{(ax^*+by^*+c)^3} + \frac{4b^2py^*+bpc}{(ax^*+by^*+c)^3} - \frac{3pb^2y^*(by^*+c)}{(ax^*+by^*+c)^4}, \\
a_{03} &= \frac{-rk^3x^*}{6(1+ky^*)^2} - \frac{pb^2x^*(ax^*+c)}{2(ax^*+by^*+c)^4}, & b_{10} &= \frac{upy^*(by^*+c)}{(ax^*+by^*+c)^2}, \\
b_{01} &= -d_2 + \frac{upx^*(ax^*+c)}{(ax^*+by^*+c)^2} - \frac{n_1qE^2}{(n_1E+n_2y^*)^2}, & b_{20} &= \frac{-aupy^*(by^*+c)}{(ax^*+by^*+c)^3}, \\
b_{11} &= \frac{2upby^*+upc}{(ax^*+by^*+c)^2} - \frac{2upby^*(by^*+c)}{(ax^*+by^*+c)^3}, & b_{02} &= \frac{-upbx^*(ax^*+c)}{(ax^*+by^*+c)^3} + \frac{n_1n_2qE^2}{(n_1+n_2y^*)^3}, \\
b_{21} &= \frac{-2aupby^*-aupc}{3(ax^*+by^*+c)^3} + \frac{abupy^*(by^*+c)}{(ax^*+by^*+c)^4}, & b_{30} &= \frac{3a^2upy^*(by^*+c)}{(ax^*+by^*+c)^4}, \\
b_{12} &= \frac{upb}{(ax^*+by^*+c)^2} - \frac{(2upby^*+upc)b}{(ax^*+by^*+c)^3} - \frac{2upb^2y^*+upbc}{(ax^*+by^*+c)^3} - \frac{3upb^2y^*(by^*+c)}{(ax^*+by^*+c)^4}, \\
b_{03} &= \frac{upb^2x^*(ax^*+c)}{(ax^*+by^*+c)^4} - \frac{n_1n_2qE^2}{(n_1E+n_2y^*)^4}, \\
P(u, v) &= \sum_{i+j=4}^{+\infty} a_{ij}u^i v^j, & Q(u, v) &= \sum_{i+j=4}^{+\infty} b_{ij}^4 u^i v^j.
\end{aligned}$$

Hence the first Lyapunov number σ for a planar system is given by

$$\begin{aligned}
\sigma &= -\frac{3\pi}{2a_{01}\Delta^{\frac{3}{2}}} \{ [a_{10}b_{10}(a_{11}^2 + a_{11}b_{02} + a_{02}b_{11}) + a_{10}a_{01}(b_{11}^2 + a_{20}b_{11} + a_{11}b_{02}) + b_{10}^2(a_{11}a_{02} + 2a_{02}b_{02}) \\
&\quad - 2a_{10}b_{10}(b_{02}^2 - a_{20}a_{02}) - 2a_{10}a_{01}(a_{20}^2 - b_{20}b_{02}) - a_{01}^2(2a_{20}b_{20} + b_{11}b_{20}) \\
&\quad + (a_{01}b_{10} - 2a_{10}^2)(b_{11}b_{02} - a_{11}a_{20})] - (a_{10}^2 + a_{01}b_{10})[3(b_{10}b_{03} - a_{01}a_{30}) + 2a_{10}(a_{21} + b_{12}) \\
&\quad + (b_{10}a_{21} - a_{01}b_{21})] \},
\end{aligned}$$

where $\Delta = a_{10}b_{01} - a_{01}b_{10}$.

If $\sigma < 0$, the Hopf bifurcation is supercritical, and the Hopf bifurcation is subcritical when $\sigma > 0$.

3. ANALYSIS OF THE MODEL IN PRESENCE OF DELAY

Letting $x = X + x^*$ and $y = Y + y^*$, after linearization, the model (1.3) could be expressed as the following form:

$$\begin{aligned}\frac{dX}{dt} &= b_1X + b_2Y, \\ \frac{dY}{dt} &= b_3X(t - \tau) + b_4Y((t - \tau)) + b_5Y,\end{aligned}$$

where

$$\begin{aligned}b_1 &= \frac{r}{1 + ky^*} - d_1 - 2\delta x^* - \frac{py^*(by^* + c)}{(ax^* + by^* + c)^2}, & b_2 &= \frac{-rkx^*}{(1 + ky^*)^2} - \frac{px^*(ax^* + c)}{(ax^* + by^* + c)^2}, \\ b_3 &= \frac{upy^*(by^* + c)}{(ax^* + by^* + c)^2}, & b_4 &= \frac{upx^*(ay^* + c)}{(ax^* + by^* + c)^2}, & b_5 &= -d_2 - \frac{qn_1E^2}{(n_1E + n_2y^*)^2}.\end{aligned}$$

Further, by calculation, we obtain the characteristic equation of the linearized system as follows:

$$\lambda^2 + A_0\lambda + B_0 + (C_0\lambda + D_0)e^{-\lambda\tau} = 0, \quad (3.1)$$

where $A_0 = -b_1 - b_5$, $B_0 = b_1b_5$, $C_0 = -b_4$, $D_0 = b_1b_4 - b_2b_3$.

Case (i) $\tau = 0$.

In absence of delay, the characteristic Eq. (3.1) becomes

$$\lambda^2 + (A_0 + C_0)\lambda + B_0 + D_0 = 0. \quad (3.2)$$

Obviously, the interior equilibrium $E^*(x^*, y^*)$ is locally asymptotically stable if and only if the root of Eq. (3.2) is negative in real part, i.e. the following conditions hold

- (a) $A_0 + C_0 > 0$,
- (b) $B_0 + D_0 > 0$.

Case (ii) $\tau \neq 0$.

As for the delayed model (1.3), the stability of positive interior equilibrium point E^* depends on the sign of the real parts of the roots of the corresponding characteristic Eq. (3.1): if the real part of all roots are negative, then the system is locally asymptotically stable around the positive interior equilibrium point E^* , otherwise it is unstable. When τ exists, substituting $\lambda = \xi + i\omega$ into the characteristic Eq. (3.1), we get

$$(\xi + i\omega)^2 + A_0(\xi + i\omega) + B_0 + (C_0(\xi + i\omega) + D_0)e^{-(\xi + i\omega)\tau} = 0. \quad (3.3)$$

Now substituting the real part $\xi = 0$, the above equation reduces to

$$-\omega^2 + A_0\omega i + B_0 + (C_0\omega i + D_0)e^{-i\omega\tau} = 0. \quad (3.4)$$

After separating the real and imaginary parts, we get in the following form:

$$\begin{aligned} D_0\cos\omega\tau + C_0\omega\sin\omega\tau &= \omega^2 - B_0, \\ C_0\omega\cos\omega\tau - D_0\sin\omega\tau &= -A_0\omega. \end{aligned} \quad (3.5)$$

Squaring and adding the above two equations, we have a bi-quadratic equation of ω ,

$$\omega^4 + (A_0^2 - C_0^2 - 2B_0)\omega^2 + (B_0^2 - D_0^2) = 0. \quad (3.6)$$

Taking $\theta = \omega^2$, $k_1 = A_0^2 - C_0^2 - 2B_0$, $k_2 = B_0^2 - D_0^2$, then the bi-quadratic Eq. (3.6) can be written as

$$\theta^2 + k_1\theta + k_2 = 0. \quad (3.7)$$

Clearly, if $k_1 > 0$ and $k_2 > 0$, then Eq. (3.7) does not contain any positive real root, that is, Equation (3.6) does not have a positive real ω . As a result, the positive equilibrium point E^* is locally asymptotically stable for any $\tau \geq 0$.

However, if $k_2 < 0$ or $k_1 < 0$, $k_2 > 0$ and $\Delta = k_1^2 - 4k_2 = 0$, then the Eq. (3.7) has one positive real root θ^* . Thus, $\omega^* = \sqrt{\theta^*}$ is the positive root of Eq. (3.6). This means that we can find a threshold value τ^* , such that $\xi(\tau^*) = 0$ and $\omega(\tau^*) = \omega^*$.

If $k_1 < 0$, $k_2 > 0$ and $\Delta = k_1^2 - 4k_2 > 0$ then the Eq.(3.7) exists two positive real roots θ_1^* and θ_2^* . Thus, $\omega_i^* = \sqrt{\theta_i^*}$ ($i = 1, 2$) are the positive roots of Eq. (3.6). This means that we can find two threshold values τ_i^* ($i = 1, 2$), such that $\xi(\tau_i^*) = 0$ and $\omega_i(\tau_i^*) = \omega_i^*$, $i = 1, 2$.

Without loss of generality, we suppose that Eq.(3.7) has two positive roots θ_i^* , ($i = 1, 2$), and let $\omega_i^* = \sqrt{\theta_i^*}$, ($i = 1, 2$). Then, from the Eq. (3.5) we can get

$$\tau_i^k = \frac{1}{\omega_i^*} \arccos \left[\frac{((\omega_i^*)^2 - B_0)D_0 - A_0C_0(\omega_i^*)^2}{D_0^2 + C_0^2(\omega_i^*)^2} \right] + \frac{2k\pi}{\omega_i^*}, i = 1, 2, k = 0, 1, 2, \dots \quad (3.8)$$

Let $\tau^* = \min \{ \tau_i^k \} (i = 1, 2, k = 0, 1, 2, \dots)$, then we verify the transversality condition. Differentiating the Eq. (3.4) with respect to τ , we get

$$\left(\frac{d\lambda}{d\tau} \right)^{-1} = \frac{2\lambda + A_0}{\lambda(\lambda^2 + A_0\lambda + B_0)} + \frac{C_0}{\lambda(C_0\lambda + D_0)} - \frac{\tau}{\lambda}, \quad (3.9)$$

thus,

$$\operatorname{Re} \left(\frac{d\lambda}{dE} \right)^{-1} \Big|_{\tau=\tau^*} = \frac{2(\omega^*)^4 + (A_0^2 - C_0^2 - 2B_0)(\omega^*)^2}{D_0^2 + C_0^2(\omega^*)^2} = \frac{2(\omega^*)^4 + k_1(\omega^*)^2}{D_0^2 + C_0^2(\omega^*)^2}. \quad (3.10)$$

The transversality condition holds at $\tau = \tau^*$ if $2(\omega^*)^4 + k_1(\omega^*)^2 \neq 0$. Hence, the model (1.3) undergoes a Hopf bifurcation at positive equilibrium point E^* when the gestation delay parameter τ crosses the threshold value τ^* . We conclude these results in the following theorem.

Theorem 3.1. *For model (1.3) with gestation delay, we have the following conclusions:*

1. *If $k_1 > 0$ and $k_2 > 0$ the positive equilibrium point E^* of model (1.3) is locally asymptotically stable for any $\tau > 0$.*

2. *If one of the following conditions:*

(i) $k_2 < 0$;

(ii) $k_1 < 0, k_2 > 0$ and $\Delta = k_1^2 - 4k_2 = 0$;

(iii) $k_1 < 0, k_2 > 0$ and $\Delta = k_1^2 - 4k_2 > 0$,

and $2(\omega^)^4 + k_1(\omega^*)^2 \neq 0$ hold, the model (1.3) undergoes a Hopf bifurcation at positive equilibrium point E^* when the gestation delay parameter τ crosses the threshold value τ^* , which means the positive equilibrium point E^* is locally asymptotically stable for $0 \leq \tau < \tau^*$ and unstable for $\tau > \tau^*$.*

4. NUMERICAL SIMULATIONS

In this section, we will use Matlab numerical simulations to validate the theoretical results obtained in the previous sections and to illustrate the effect of the predator interference constant b , non-linear harvesting and the delay τ on the dynamic behavior of the model (1.3), respectively. Therefore, in this section, our analysis will be carried out by two different parts: (a) analysis for $\tau = 0$, i.e., for non-delayed system, (b) analysis for different values of τ , i.e., analysis for delayed system.

4.1. Numerical analysis for non-delayed system ($\tau = 0$). In this subsection, we discuss how changing the biologically significant parameters b and E , respectively, affects the dynamics of the system (1.2).

Firstly, in order to verify the presence of positive equilibrium points in the system (1.2), we use the harvesting effort coefficient E as a parameter to count the number of equilibrium points within the system. In fig. 1, we observe that when the parameter condition $a_6 > 0$ is satisfied, there exist a different number of internal equilibrium points as the parameter E varies. figs. 1a to 1d show that the system can have two distinct interior equilibrium points, a unique coincident internal equilibrium point, and no interior equilibrium point. However, when the parameter satisfies $a_6 < 0$, as shown in fig. 2, we have presented that changing the value of the parameter E does not affect the number of internal equilibrium points.

Secondly, in order to verify the stability of each equilibrium point of the model (1.2), the parameters satisfying the theorem are selected, and the numerical simulation results verify the correctness of the theory. fig. 3 clearly shows that when the parameter condition is satisfied by $r > d_1$, both predators and prey tend to become extinct. fig. 4 shows that the equilibrium point E_1 is locally asymptotically stable when the parameters satisfy certain conditions, i.e., in this case, the predator tends to become extinct. In fig. 5, it is easy to obtain the local asymptotic stability of the positive equilibrium point of the model (1.2).

Now, two important parameters in the model (1.2) are analyzed, namely the inter-predator interference constant b and the harvesting effort of the predator E . fig. 6 shows the bifurcation diagram of system (1.2) with regard to b . The system (1.2) undergoes a Hopf bifurcation when the value of b is changed from 0 to 3, as seen in this diagram. From $0 \leq b < 1.468$, the system (1.2) exhibits oscillating behavior, whereas for $1.468 \leq b \leq 3$, the system (1.2) exhibits stable steady state behavior. From a biological point of view, this behavior makes sense. Because of increased inter-predator interference, predator and prey densities are maintained at a certain level, allowing the coexistence of both species. Therefore, it shows that the mutual interference of predators may be the cause of system stability.

Then, we analyze the effect of the harvest effort value parameter E on the dynamical behavior of the model (1.2). Bifurcation diagram of system (1.2) with respect to E is plotted in

fig. 7. From this figure, it is seen that by increasing the strength of E , above the threshold value $E_{HB}^1(0.0009341)$ the interior equilibrium point loses its stability, and the populations of prey and predator show periodic oscillations. Therefore, the system (1.2) undergoes a Hopf bifurcation at $E_{HB}^1 = 0.0009341$. Further, the value of E is continuously increasing. When the value of E exceeds $E_{HB}^2(0.02218)$, the system (1.2) becomes stable from periodic oscillation. So, the system (1.2) undergoes another Hopf bifurcation at $E_{HB}^2 = 0.02218$. Therefore, the system (1.2) exhibits multiple Hopf bifurcations at $E_{HB}^1 = 0.0009341$ and $E_{HB}^2 = 0.02218$, respectively, and shows periodic oscillation when the harvesting effort is in the middle. Four different phase diagrams for different E values, such as before the first Hopf bifurcation, between two Hopf bifurcations and after the second bifurcation, are given in figs. 8a to 8d. The biological significance of the parameter harvesting effort E is that the system shows switching behaviour with respect to the parameter E , which is most important in the biological aspect.

When we use the parameters from Pal et al. [20], we observe that the system (1.2) experiences Hopf bifurcation twice with respect to the fear effect parameter k for threshold values $k_{HB}^1 = 0.3139$ and $k_{HB}^2 = 0.9205$. Bifurcation diagram of system (1.2) with respect to k is plotted in fig. 9. Interestingly, we observed that this phenomenon is consistent with that obtained by Pal et al. [20]. Similarly, we can obtain that fear of predation risk can have both a stabilizing and destabilizing effect, which plays an important role in the ecosystem.

4.2. Numerical analysis for delayed system ($\tau > 0$). In this section, we study the dynamic behavior of model (1.3) and simulate the effect of time delay τ on the stability of the interior equilibrium point E^* . Bifurcation diagram of system (1.3) with respect to τ has been drawn in fig. 10. It is seen that the delay-induced model (1.3) undergoes a Hopf bifurcation around the positive equilibrium point E^* for the threshold value $\tau^* = 1.441$. As a result, when $\tau < \tau^*$, the model (1.3) is stable around the positive equilibrium point E^* and unstable when $\tau > \tau^*$. fig. 11 also shows that the model (1.3) is stable for $\tau = 1.2 < \tau^*$ and unstable for $\tau = 1.58 > \tau^*$. Therefore, it can be concluded that the time delay has an important effect on the dynamics of the model.

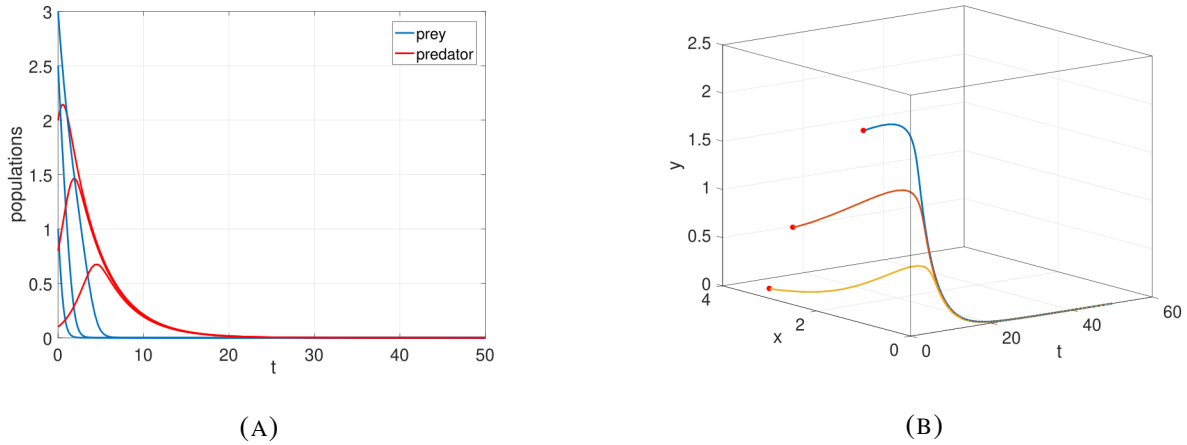


FIGURE 3. Local stability of trivial equilibrium point $E_0(0,0)$ of model (1.2) for the set of parametric values $r = 0.01$, $k = 30$, $d_1 = 0.05$, $\delta = 0.1$, $p = 2$, $a = 1.5$, $b = 2.5$, $c = 0.3$, $d_2 = 0.1$, $u = 0.7$, $q = 0.8$, $E = 1.5$, $n_1 = 5$, $n_2 = 0.2$. Red dots indicate the initial point of the trajectory. The initial conditions are $(1, 2)$, $(2.5, 0.8)$ and $(3, 0.1)$.

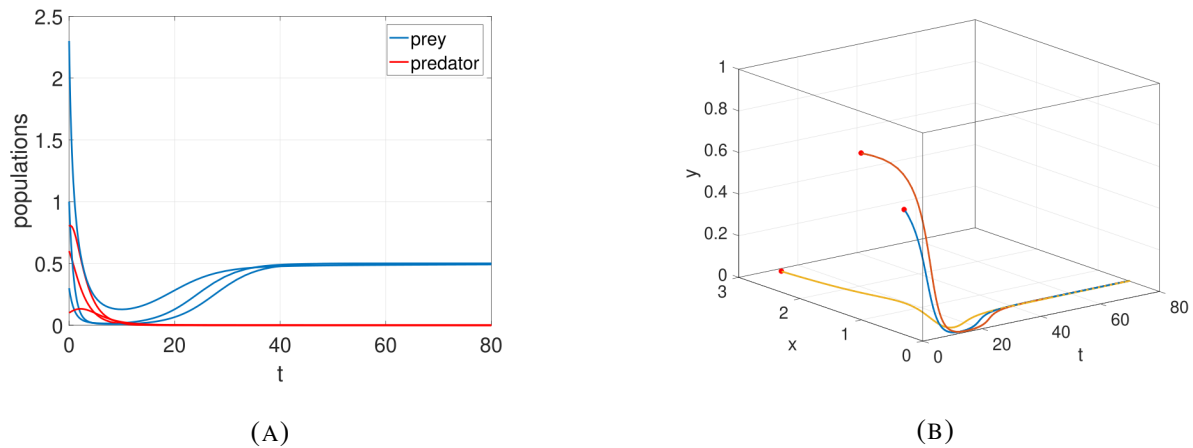


FIGURE 4. Local stability of predator-free equilibrium point $E_1(0.5,0)$ of model (1.2) for the set of parametric values $r = 0.3$, $k = 30$, $d_1 = 0.05$, $\delta = 0.5$, $p = 2$, $a = 1.5$, $b = 0.5$, $c = 0.82$, $d_2 = 0.1$, $u = 0.7$, $q = 1.8$, $E = 1.5$, $n_1 = 5$, $n_2 = 0.2$. Red dots indicate the initial point of the trajectory. The initial conditions are $(0.3, 0.6)$, $(1, 0.8)$ and $(2.3, 0.1)$.

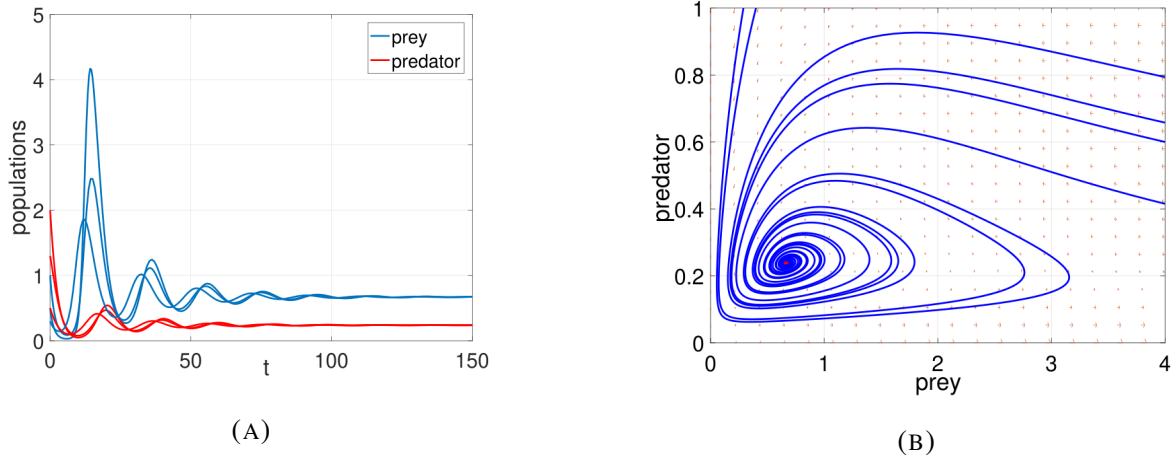


FIGURE 5. Local stability of the interior equilibrium point $E^* = (0.67118, 0.23855)$ of model (1.2) for the set of parametric values $r = 3$, $k = 30$, $d_1 = 0.05$, $\delta = 0.1$, $p = 2$, $a = 1.5$, $b = 2.5$, $c = 0.3$, $d_2 = 0.1$, $u = 0.7$, $q = 0.8$, $E = 1.5$, $n_1 = 2$, $n_2 = 0.2$.

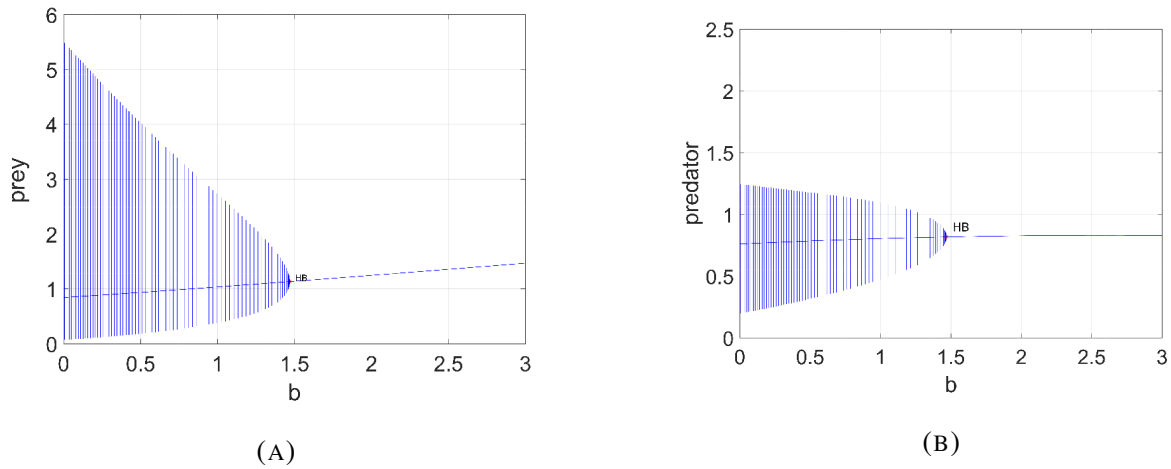
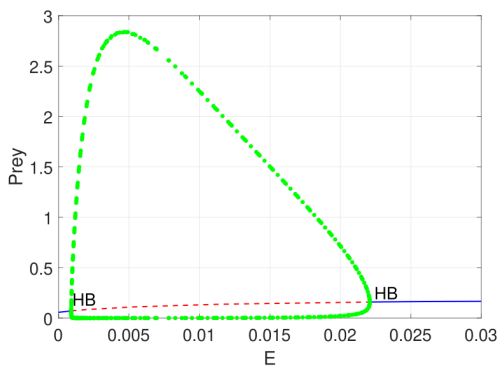
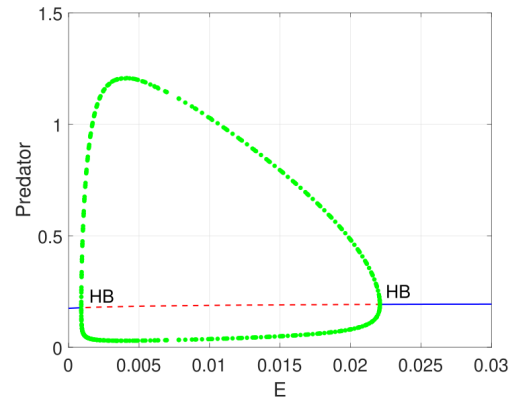


FIGURE 6. Bifurcation diagram of the system (1.2) with respect to b of prey and predator by taking the parametric values $r = 1$, $k = 2.5$, $d_1 = 0.05$, $\delta = 0.1$, $p = 2$, $a = 5$, $c = 3$, $d_2 = 0.1$, $u = 0.7$, $q = 0.8$, $E = 0.2$, $n_1 = 5$, $n_2 = 2$.



(A)



(B)

FIGURE 7. Bifurcation diagram of the system (1.2) with respect to E of prey and predator by taking the parametric values $r = 3$, $k = 30$, $d_1 = 0.05$, $\delta = 0.1$, $p = 2$, $a = 1.5$, $b = 2.5$, $c = 0.3$, $d_2 = 0.1$, $u = 0.7$, $q = 0.8$, $n_1 = 5$, $n_2 = 0.2$.

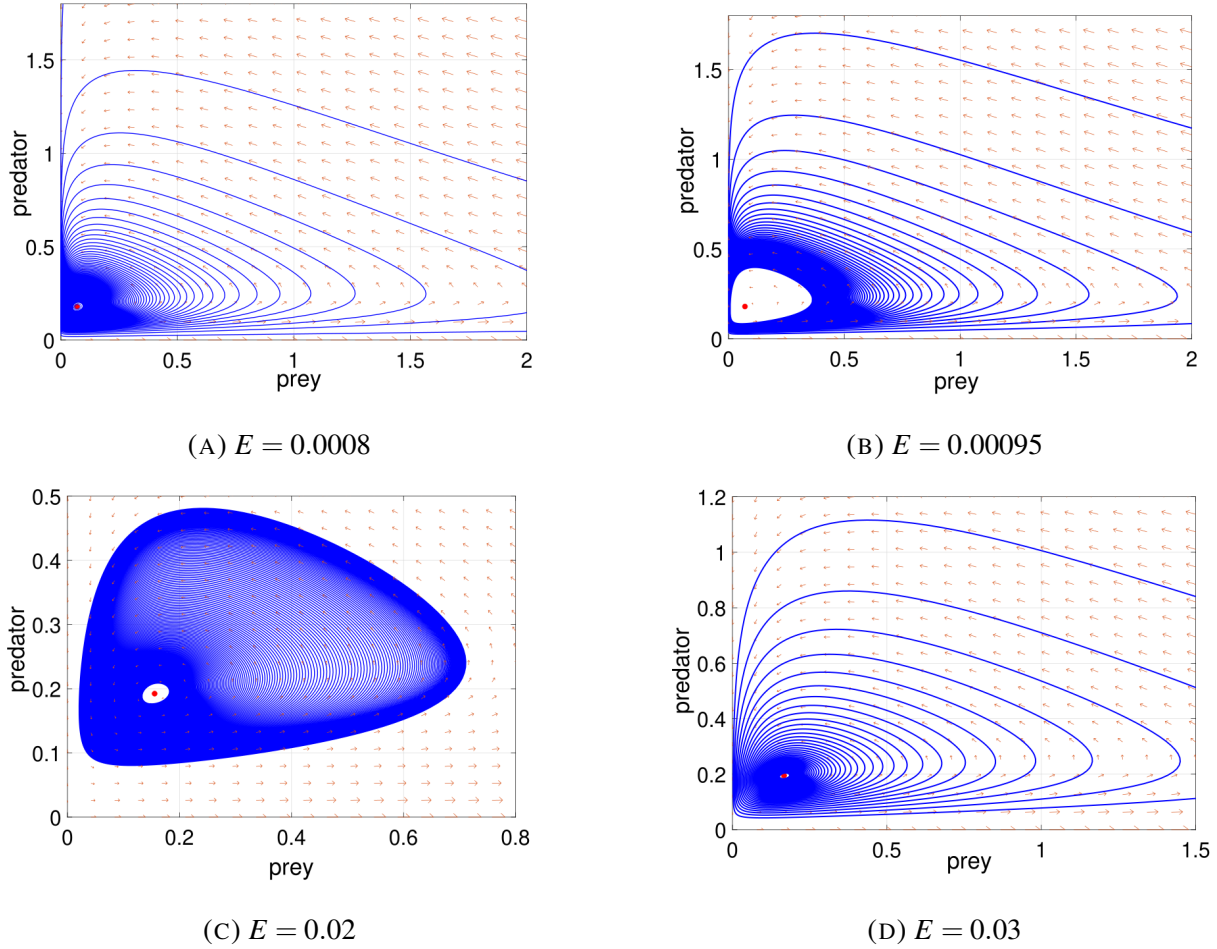


FIGURE 8. Phase diagram for three different values of harvesting effort parameter E of the model system (1.2) such as: (a) $E = 0.0008$ for stable interior equilibrium point, (b) the system (1.2) exhibits limit cycles for $E = 0.00095$, (c) the system (1.2) exhibits multiple limit cycles for $E = 0.02$, (d) $E = 0.03$ for stable interior equilibrium point, where other parameters are $r = 3$, $k = 30$, $d_1 = 0.05$, $\delta = 0.1$, $p = 2$, $a = 1.5$, $b = 2.5$, $c = 0.3$, $d_2 = 0.1$, $u = 0.7$, $q = 0.8$, $n_1 = 5$, $n_2 = 0.2$

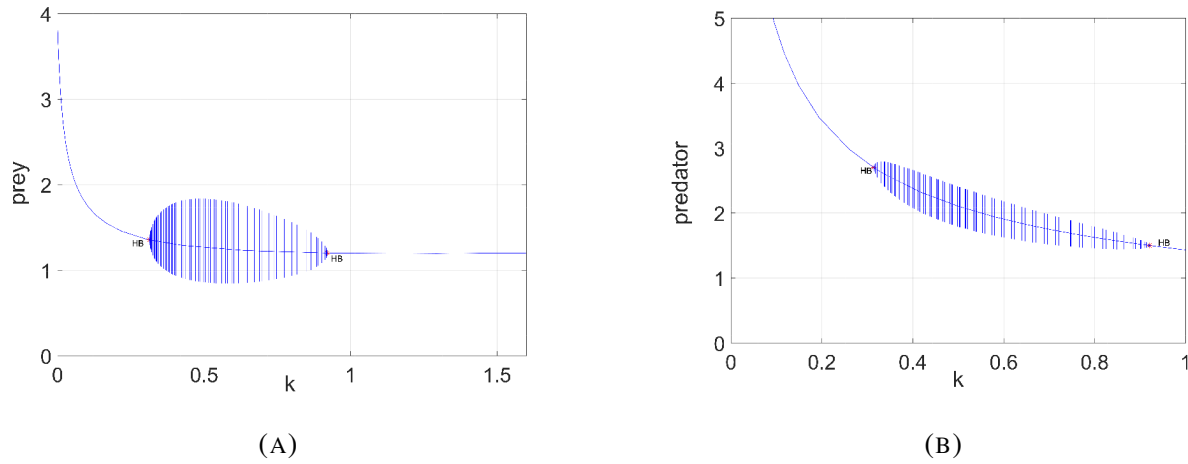


FIGURE 9. Bifurcation diagram of system (1.3) has been drawn with respect to k of prey and predator by taking the parametric values $r = 1$, $k = 2.5$, $d_1 = 0.05$, $\delta = 0.1$, $p = 2$, $a = 5$, $b = 2$, $c = 3$, $d_2 = 0.1$, $u = 0.7$, $q = 0.8$, $E = 0.2$, $n_1 = 5$, $n_2 = 2$.

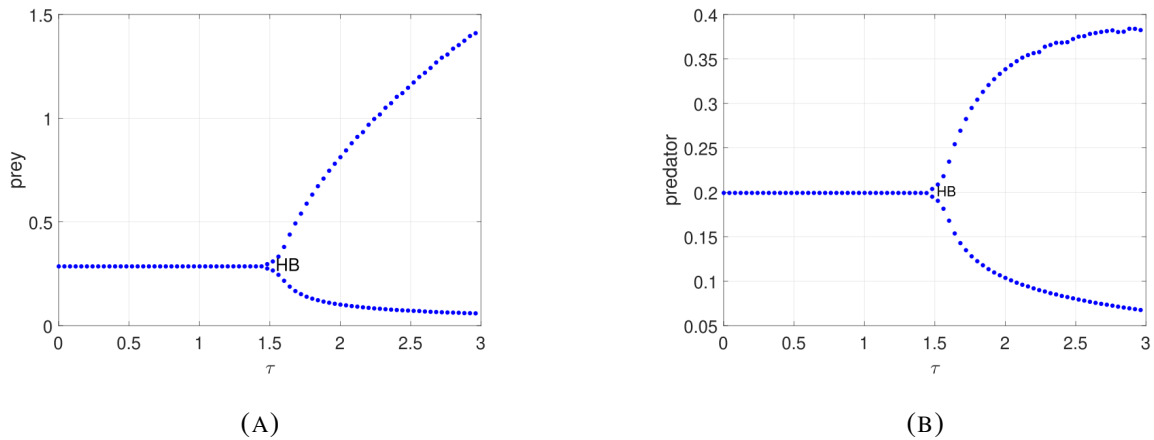


FIGURE 10. Bifurcation diagram of system (1.3) has been drawn with respect to τ of prey and predator by taking the parametric values $r = 3$, $k = 30$, $d_1 = 0.05$, $\delta = 0.8$, $p = 2$, $a = 0.5$, $b = 2$, $c = 0.3$, $d_2 = 0.1$, $u = 0.7$, $q = 0.8$, $E = 0.3$, $n_1 = 2$, $n_2 = 0.2$.

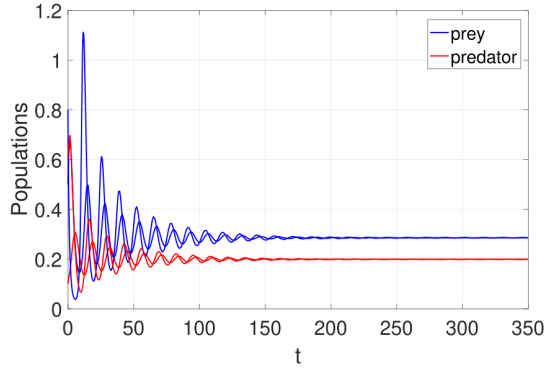
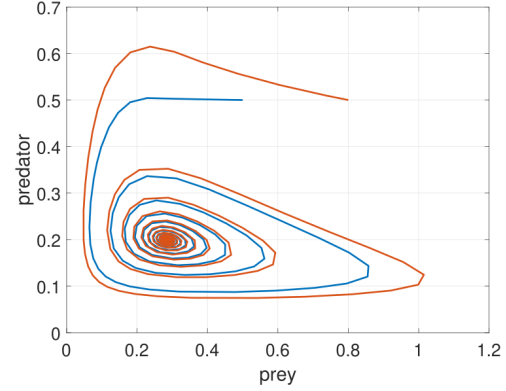
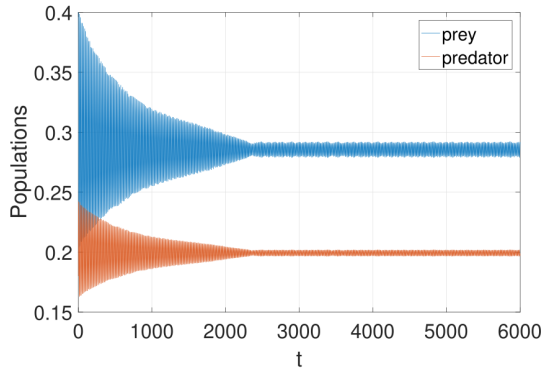
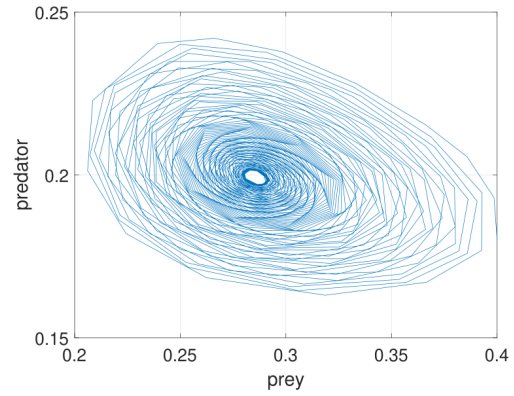
(A) $\tau = 1.2$ (B) $\tau = 1.2$ (C) $\tau = 1.58$ (D) $\tau = 1.58$

FIGURE 11. Time evolution and phase portrait of model (1.3) with time delay τ , (a) E^* is stable for $\tau = 1.2$, (b) E^* is unstable for $\tau = 1.58$ and other parameter values are $r = 3$, $k = 30$, $d_1 = 0.05$, $\delta = 0.8$, $p = 2$, $a = 0.5$, $b = 2$, $c = 0.3$, $d_2 = 0.1$, $u = 0.7$, $q = 0.8$, $E = 0.3$, $n_1 = 2$, $n_2 = 0.2$.

5. CONCLUSION

In this present article, a model of prey and predator interaction is developed. The assumption is that the fear factor is thought to influence the pace of prey growth. It is assumed that predator consumes prey according to Beddington-DeAngelis functional response. In addition, predators are economically important and non-linear harvesting strategies are used. Further, we introduced a gestation delay in the system to obtain more realistic and richer dynamics.

Firstly, we study the model dynamics without introducing the delay parameter. We validate

the positivity and boundedness of solutions of system. Three different types of equilibrium points for the system are calculated, i.e., the trivial equilibrium point (E_0), the predator-free equilibrium point (E_1), and the coexistence equilibrium point (E^*). Furthermore, for different parameter conditions, the local stability at all equilibrium points is discussed by eigenvalue analysis method. By choosing the birth rate of prey population r as the bifurcation parameter, model (1.2) undergoes a transcritical bifurcation at the trivial equilibrium point $E_0(0,0)$ when r passes through the threshold value $r^{[TC]}$. Similarly, by choosing the maximum predation rate p as the bifurcation parameter, the transcritical bifurcation is experienced at the predator-free equilibrium point $E_1(\frac{r-d_1}{\delta}, 0)$ when p passes the threshold $p^{[TC]}$. The theoretical analysis shows that when the harvest effort parameter E is chosen as the bifurcation parameter, the model (1.2) undergoes a Hopf bifurcation near the positive equilibrium point E^* . Further, we calculate the first Lyapunov number based on the normal form theory and determined the direction of the Hopf bifurcation. Numerical simulations show that the system exhibits periodic oscillations when the mutual interference coefficient of predators is small ($b < b_{HB}$), while it is stable when it crosses the threshold b_{HB} . In other words, an appropriate increase in mutual interference between predators contributes to the coexistence of both species. Additionally, numerical simulations show that for lower values of harvest effort ($E < E_{HB}^1$), the system exhibits stable dynamics; for moderate values of harvest effort ($E_{HB}^1 < E < E_{HB}^2$), the system show periodic oscillations; and for higher values of harvest effort ($E > E_{HB}^2$), the system exhibits stable dynamics (see fig. 7). Both the switching of stability occurs via Hopf bifurcation. Again, we find that the limit cycle of the system is stable. An interesting finding is that the system (1.2) also has multiple Hopf bifurcations at $k_{HB}^1 = 0.3139$ and $k_{HB}^2 = 0.9205$, respectively. Thus, harvesting efforts and fear effects can have both stabilizing and destructive effects and play an important role in ecosystem stability. From a biological point of view, this behavior makes perfect sense because predator and prey densities are maintained at a certain level for the coexistence of both species only when harvest effort is low ($E < E_{HB}^1$) or when harvest effort is above the second harvest limit ($E > E_{HB}^2$). Therefore, for the survival of these two species, businessmen must be conscious of not fishing within the two harvest limits.

Secondly, in the delayed system we observe that the delay parameter(τ) has a high impact

on dynamics of the system (1.3). By choosing the time delay τ as the bifurcation parameter, Hopf bifurcation occurs near the positive equilibrium point E^* when the time delay parameter τ exceeds a threshold value τ^* (see fig. 10). Furthermore, we discover that the system is locally asymptotically stable at the positive equilibrium point when $\tau < \tau^*$ and locally unstable when $\tau > \tau^*$ by selecting appropriate parameter values.

Pal et al. [20] considered a predator-prey system without nonlinear harvesting, and they found that the system showed two Hopf bifurcation points when fear level was chosen as the bifurcation parameter. Our study find that the system of model (1.2) also shows multiple Hopf bifurcations when k is chosen as the bifurcation parameter after the introduction of nonlinear harvesting. Furthermore, when predator mutual interference coefficient b and harvest effort value E are used as bifurcation parameters, model (1.2) shows one Hopf bifurcation point and two Hopf bifurcation points, respectively. In addition, it is more realistic and easier to observe biological diversity by considering nonlinear capture than the predator-prey model with linear harvest proposed by Majumdar et al. [21]. Finally, the proposed model is applicable to marine subecosystems where harvesting provides financial support.

ACKNOWLEDGEMENTS

This work is supported by the Natural Science Foundation of China (11672074), and the Natural Science Foundation of Fujian Province (2022J01192).

CONFLICT OF INTERESTS

The authors declare that there is no conflict of interests.

REFERENCES

- [1] A.J. Lotka, Elements of physical biology, Williams and Wilkins Company, Baltimore, 1925.
- [2] J.B. Collings, The effects of the functional response on the bifurcation behavior of a mite predator-prey interaction model, *J. Math. Biol.* 36 (1997), 149–168. <https://doi.org/10.1007/s002850050095>.
- [3] H. Zhang, Y. Cai, S. Fu, et al. Impact of the fear effect in a prey-predator model incorporating a prey refuge, *Appl. Math. Comput.* 356 (2019), 328–337. <https://doi.org/10.1016/j.amc.2019.03.034>.
- [4] K. Sarkar, S. Khajanchi, Impact of fear effect on the growth of prey in a predator-prey interaction model, *Ecol. Complex.* 42 (2020), 100826. <https://doi.org/10.1016/j.ecocom.2020.100826>.

- [5] S. Jawad, Study the dynamics of commensalism interaction with Michaelis-Menten type prey harvesting, *Al-Nahrain J. Sci.* 25 (2022), 45–50.
- [6] C.S. Holling, The functional response of predators to prey density and its role in mimicry and population regulation, *Mem. Entomol. Soc. Can.* 97 (1965), 5–60. <https://doi.org/10.4039/entm9745fv>.
- [7] A.Y. Morozov, Emergence of Holling type III zooplankton functional response: Bringing together field evidence and mathematical modelling, *J. Theor. Biol.* 265 (2010), 45–54. <https://doi.org/10.1016/j.jtbi.2010.04.016>.
- [8] P.A. Abrams, L.R. Ginzburg, The nature of predation: prey dependent, ratio dependent or neither?, *Trends Ecol. Evol.* 15 (2000), 337–341. [https://doi.org/10.1016/s0169-5347\(00\)01908-x](https://doi.org/10.1016/s0169-5347(00)01908-x).
- [9] R. Arditi, N. Perrin, H. Saïah, et al. Functional responses and heterogeneities: An experimental test with cladocerans, *Oikos* 60 (1991), 69–75. <https://doi.org/10.2307/3544994>.
- [10] A.P. Gutierrez, Physiological basis of ratio-dependent predator-prey theory: The metabolic pool model as a paradigm, *Ecology*. 73 (1992), 1552–1563. <https://doi.org/10.2307/1940008>.
- [11] R. Arditi, H.R. Akçakaya, Underestimation of mutual interference of predators, *Oecologia*. 83 (1990), 358–361. <https://doi.org/10.1007/bf00317560>.
- [12] C. Jost, S.P. Ellner, Testing for predator dependence in predator-prey dynamics: a non-parametric approach, *Proc. R. Soc. Lond. B* 267 (2000), 1611–1620. <https://doi.org/10.1098/rspb.2000.1186>.
- [13] C. Jost, R. Arditi, From pattern to process: identifying predator-prey models from time-series data, *Popul. Ecol.* 43 (2001), 229–243. <https://doi.org/10.1007/s10144-001-8187-3>.
- [14] J.R. Beddington, Mutual interference between parasites or predators and its effect on searching efficiency, *J. Animal Ecol.* 44 (1975), 331–340. <https://doi.org/10.2307/3866>.
- [15] D.L. DeAngelis, R.A. Goldstein, R.V. O’Neill, A model for trophic interaction, *Ecology*, 56 (1975), 881–892. <https://cir.nii.ac.jp/crid/1570009750691906560>.
- [16] L.Y. Zanette, A.F. White, M.C. Allen, et al. Perceived predation risk reduces the number of offspring songbirds produce per year, *Science*. 334 (2011), 1398–1401. <https://doi.org/10.1126/science.1210908>.
- [17] X. Wang, L. Zanette, X. Zou, Modelling the fear effect in predator-prey interactions, *J. Math. Biol.* 73 (2016), 1179–1204. <https://doi.org/10.1007/s00285-016-0989-1>.
- [18] A.A. Thirthar, S.J. Majeed, M.A. Alqudah, et al. Fear effect in a predator-prey model with additional food, prey refuge and harvesting on super predator, *Chaos Solitons Fractals* 159 (2022), 112091. <https://doi.org/10.1016/j.chaos.2022.112091>.
- [19] D. Hu, H. Cao, Stability and bifurcation analysis in a predator-prey system with Michaelis-Menten type predator harvesting, *Nonlinear Anal.: Real World Appl.* 33 (2017), 58–82. <https://doi.org/10.1016/j.nonrwa.2016.05.010>.

- [20] S. Pal, S. Majhi, S. Mandal, et al. Role of fear in a predator–prey model with Beddington–DeAngelis functional response, *Z. Naturforsch., A.* 74 (2019), 581–595. <https://doi.org/10.1515/zna-2018-0449>.
- [21] P. Majumdar, B. Mondal, S. Debnath, et al. Effect of fear and delay on a prey–predator model with predator harvesting, *Comput. Appl. Math.* 41 (2022), 357. <https://doi.org/10.1007/s40314-022-02066-z>.